Electric double-layer potentials and surface regulation properties measured by colloidal-probe atomic force microscopy

Montes Ruiz-Cabello, F. Javier; Trefalt, Gregor; Maroni, Plinio; Borkovec, Michal

How to cite

MONTES RUIZ-CABELLO, F. Javier et al. Electric double-layer potentials and surface regulation properties measured by colloidal-probe atomic force microscopy. In: Physical Review. E, 2014, vol. 90, n° 012301. doi: 10.1103/PhysRevE.90.012301

This publication URL: https://archive-ouverte.unige.ch/unige:143904
Publication DOI: 10.1103/PhysRevE.90.012301

PHYSICAL REVIEW E **90**, 012301 (2014)

Electric double-layer potentials and surface regulation properties measured by colloidal-probe atomic force microscopy

F. Javier Montes Ruiz-Cabello, Gregor Trefalt, Plinio Maroni, and Michal Borkovec[*]
Department of Inorganic and Analytical Chemistry, University of Geneva, Sciences II, Quai Ernest-Ansermet 30, 1205 Geneva, Switzerland
(Received 17 April 2014; published 2 July 2014)

We show how the colloidal-probe technique, which is based on force measurements made with the atomic force microscope, can be used to accurately determine the charging parameters of water-solid interfaces. Besides yielding accurate values of the double-layer or diffuse-layer potential, the method also allows reliable determination of the charge regulation properties of the surfaces. The latter can be quantified with a regulation parameter, which is essential to properly describe forces between interfaces, especially in asymmetric situations when one of the interfaces is charged and the other one is close to neutral. The technique relies on a highly charged probe particle, for which the charging properties are accurately determined by interpreting the double-layer contribution of the measured force profiles in the symmetric sphere-sphere geometry with Poisson-Boltzmann (PB) theory. Once the probe particle is calibrated, this particle is used to measure the force profile between an unknown substrate in the asymmetric sphere-sphere or sphere-plane geometry. From this profile, the diffuse-layer potential and regulation parameter of the substrate can be again determined with PB theory. The technique is highly versatile, as it can be used for a wide variety of substrates, including colloidal particles and planar substrates. The technique is also applicable in salt solutions containing multivalent ions. The current drawbacks of the technique are that it can only be applied up to moderately high salt levels, typically to 10 mM, and only for relatively large particles, typically down to about 1 μm in diameter. How the technique could be extended to higher salt levels and smaller particle size is also briefly discussed.

DOI: 10.1103/PhysRevE.90.012301 PACS number(s): 82.70.Dd, 82.65.+r, 07.79.Lh, 61.20.Qg

I. INTRODUCTION

Water-solid interfaces are central in soft condensed matter physics, material sciences, and environmental engineering [1–4]. Many processes are governed by interactions between such interfaces, for example, formation of colloidal photonic crystals [1], preparation of ceramic green bodies [2], or transport of colloidal particles in the subsurface [3]. In many situations, the underlying interactions involving particles and surfaces can be quantified with the theory developed by Derjaguin, Landau, Verwey, and Overbeek (DLVO) [4]. This theory stipulates that these interactions can be approximated by a superposition of van der Waals and electrical double-layer forces. Deviations from DLVO theory have been reported at shorter separation distances, and they were related to ion correlation or hydrophobic forces as well as to patchy or hairy surfaces [4–8].

Double-layer forces are normally described with the Poisson-Boltzmann (PB) theory, or its linearized version, the Debye-Hückel (DH) theory. Double-layer forces depend strongly on the solution composition and the electric surface potential. While the solution composition is usually known or can be inferred from chemical equilibrium considerations [9,10], the surface potential of water-solid interfaces depends not only on the type of material, but also on the surface composition, and on the presence of adsorbed species [4,11–13]. Moreover, the force profiles are not determined by the potential directly at the surface, which is referred to as the surface potential, but rather by the potential at the plane of origin of the diffuse layer. This potential is called the diffuse-layer potential, double-layer potential, renormalized potential, or the effective potential [4,8,14]. The diffuse-layer potential cannot be easily estimated even for the simplest materials, and must be measured.

Direct force measurements between such interfaces represent a straightforward way to measure the diffuse-layer potential. The surface forces apparatus (SFA) was the first reliable tool for such measurements, which still remains unsurpassed in distance resolution, currently <0.1 nm [15,16]. However, the SFA relies on mica as a substrate, which limits its broad applicability. The advent of the atomic force microscope (AFM) [17] soon led to the development of the more versatile colloidal-probe technique [18–20]. This method replaces the sharp AFM tip with a so-called colloidal probe, which consists of a μm-sized colloidal particle that is attached to a tipless AFM cantilever. In this fashion, forces in the sphere-plane geometry become accessible. Total internal reflection microscopy (TIRM) represents an alternative technique to measure forces between particles and planar substrates [21]. In comparison with the colloidal probe, TIRM offers better force resolution, but inferior distance resolution. By attaching colloidal particles to the substrate as well, one can also measure forces between two particles in the sphere-sphere geometry with the AFM [22–24]. With optical tweezers and videomicroscopy forces between two particles can also be accessed directly, again with superior force resolution but poorer distance resolution [25–27].

To quantify forces between charged interfaces within DH or PB theory, charge regulation properties of the interface must be known [28–32]. Many authors use the classical boundary conditions of constant charge (CC) and constant potential (CP). Recent force measurements between water-solid interfaces involving one electrically charged and another neutral interface

---

[*] Corresponding author: michal.borkovec@unige.ch

reveal that these boundary conditions can be grossly inaccurate [24]. The charge regulation capacity of the neutral interface even determines the sign of the double-layer force. Therefore, the quantification of the regulation properties becomes almost as important as the determination of the diffuse-layer potential. While the detailed treatment of charge regulation effects requires a quantification of the adsorption equilibria, one may invoke the constant regulation (CR) approximation to describe the charge regulation capacity of the interface by means of a single parameter [29,30]. This regulation parameter p provides an intuitive description of the classical boundary conditions, since $p = 1$ corresponds to CC, while $p = 0$ corresponds to CP. This CR approximation thus offers a simple way to parametrize the regulation properties of an interface by means of a single parameter. Therefore, the charging properties of an interface can be quantified with two parameters, namely, the diffuse-layer potential and the regulation parameter.

One might argue that these charging properties can be simply accessed by means of direct force measurements between the respective interfaces. However, this statement is only correct provided the sign of the diffuse-layer potential is known, and when the magnitude of the potential is sufficiently high, typically >30 mV. The sign of the potentials cannot be extracted from a simple force measurement. Moreover, when weakly charged interfaces come into play, the interaction forces are weak, and they cannot be measured with confidence. In such situations, one must also consider other types of interactions, such as van der Waals or hydrophobic forces [7,33,34]. These additional forces modify the force profiles substantially, and the respective charging parameters cannot be extracted.

Electrokinetic techniques are also widely used to determine electric potentials of surfaces. These potentials are referred to as the ζ potentials, and they were argued to be comparable to diffuse-layer potentials [4,35,36]. In spite of the simplicity of these techniques, elaborate models are often needed to analyze the data quantitatively [37–40]. The standard electrokinetic model makes assumptions concerning surface conductivity and hydrodynamic boundary conditions, especially concerning the location of the shear plane. These assumptions are difficult to verify. Under some conditions, the electrophoretic mobility further goes through a maximum as a function of the ζ potential, which makes the data inversion nonunique [35,37]. Moreover, the interaction of surface charge heterogeneities with an applied electric field may generate torques on the particles, and induce particle rotations. This rotational motion may further enhance the electrophoretic mobility and lead to an overestimation of the ζ potential [41]. These effects may also lead to electrophoretic mobilities exceeding values predicted by the standard electrokinetic model, making the data inversion impossible [36]. These effects were probably also responsible for the observations that measured ζ potentials were larger in magnitude than the diffuse-layer potentials determined from direct force measurements, especially when their magnitudes were high [7,34,42]. Given these difficulties with the quantification of the electrokinetic results, we suspect that direct force measurements provide the more reliable way to determine diffuse-layer potentials.

In the present article, we propose a variant of colloidal-probe technique that uses a highly charged probe particle with precisely known charging properties. These properties are calibrated by means of force measurements between two such particles in the symmetrical sphere-sphere geometry. This probe particle is subsequently used to determine the charging properties of another interface to be investigated, which can be another colloidal particle or a planar substrate. The substantial advantage of this technique is that it can be used to accurately measure the diffuse-layer potential and the regulation parameter even of very weakly charged substrates. Moreover, the sign of this potential can be determined unambiguously.

II. EXPERIMENT AND METHODS

A. Materials

Three different types of polystyrene latex particles were used, namely, amidine-terminated latex (AL), sulfate-terminated latex (SL), and carboxyl-terminated latex (CL). Their mean diameters and polydispersities as determined by the manufacturer (Invitrogen) are summarized in Table I. The particles were dialyzed for about 1 week against Milli-Q (Millipore) water, until the conductivity reached the value of the pure water. Particles were suspended in either in KCl, K_2SO_4, or $LaCl_3$ solutions, which were adjusted to pH 3.0 or 4.0 by HCl. Milli-Q water was used throughout. All measurements were carried out at room temperature at $22 \pm 2\,^{\circ}$C.

Silicon wafers (p-type, Silchem, Germany) were used for the particle-substrate force measurements. These wafers have a silica layer of about 1.5 nm in thickness, which results from the spontaneous oxidation of the silicon surface in air. This thickness was measured by null ellipsometry (Multiskop, Optrel). They were cleaned with piranha solution, which is a mixture of H_2SO_4 (96%) and H_2O_2 (30%) with a ratio of 3:1 for 60 min. Subsequently, they were rinsed with Milli-Q water and dried in a stream of nitrogen.

The root mean square (rms) roughness was measured by AFM imaging in intermittent contact mode in solution. The latex particles were deposited for about 1 h on a piranha-cleaned and silanized silica slide with dimensions about 1 cm × 1 cm. Silica slides were silanized overnight in an evacuated glass container aside a 50-μL drop of a silanol. For SL and CL particles 3-ethoxydimethylsilylpropylamine was used, while

TABLE I. Properties of the colloidal particles used.

Particles	Abbreviation	Diameter[a] (μm)	Polydispersity[a] (%)	Roughness[b] (nm)
Sulfate latex	SL	3.0	4.1	0.8
Carboxyl latex	CL	1.0	4.5	0.4
Amidine latex	AL	0.95	3.6	0.5

[a] Determined by transmission electron microscopy by the manufacturer.

[b] rms roughness determined by AFM.

for the AL particles (3-glycidoxypropyl)dimethylethoxysilane was used. After the deposition of the particles, the nonadsorbed particles were gently washed out with a 10 mM KCl solution. The images were recorded in liquid with a Cypher AFM instrument (Asylum Research, Santa Barbara, CA). We used BioLever Mini cantilevers (BL-AC40TS, Olympus, Japan) with a nominal tip radius <9 nm and a resonance frequency of around 30 kHz in water. The scan size was 0.5 μm × 0.5 μm, the scan rate 2.0 Hz, and the free oscillation amplitude (FOA) was 20 nm. The set point was fixed at around 70% of the FOA. The rms roughness of the particles is summarized in Table I and was always <1 nm. The rms roughness of the silicon wafer is 0.3 nm.

B. Direct force measurements

The multiparticle colloidal-probe technique was used to measure forces between particles with a closed-loop AFM (MFP-3D, Asylum Research) mounted on an inverted optical microscope (Olympus IX70) [24,43]. The glass plate sealing the fluid cell was treated with piranha solution overnight, rinsed with water, dried, and cleaned in an air-plasma for 20 min. The tipless cantilevers (MikroMasch, HQ CSC37, without Al coating) were also plasma cleaned in the same way. The glass plate and the cantilevers were silanized overnight in an evacuated container with two separate drops of 20 μL of 3-ethoxydimethylsilylpropylamine and 100 μL of (3-glycidoxypropyl)dimethylethoxysilane.

The AFM fluid cell was separated with a Teflon spacer into two compartments and the respective latex suspensions were injected into each part of the cell. The particles were left to deposit on the glass plate for 2 h. The fluid cell was then flushed with the same salt solution as the one used to prepare the latex suspension in order to exchange the liquid and to remove the remaining particles that did not attach to the substrate. To carry force measurements between two individual particles, one particle was picked up with the silanized cantilever, and the particle was centered above another particle deposited on the substrate. The lateral centering was achieved through optical fringes observed in the optical microscope with an accuracy of about 100 nm. Between one pair of particles, at least 120 vertical approach-retraction cycles were recorded with a sampling rate of 5 kHz, an approach-retraction velocity of 300 nm/s, and a cycle frequency of 0.5 Hz. The zero separation distance was determined from the onset of the constant compliance region with a precision of about 0.3 nm. The forces were obtained from the cantilever deflection recorded in the approach part of the force curves and the spring constant of the cantilever. The spring constant was measured with the thermal noise method, and the values were in the range of 0.1–0.3 N/m. Subsequent downsampling of the force curves to 150 Hz and averaging of the different approach curves yields a force resolution of about 1 pN. At least three pairs involving different particles were measured for all conditions, and good reproducibility was normally found. In particular, a measurement sequence consisted in measuring the symmetric system, then the asymmetric system, and finally the symmetric system again. Only small deviations between the successive measurements in the symmetric systems were observed, which indicated that the probe particle remained unchanged during this sequence.

Forces between latex particles and the silica substrate were measured by fixing the clean silicon wafer on the silanized glass plate in the fluid cell. A Teflon spacer was used to divide the fluid cell intro two compartments, whereby the silicon wafer was located on one side of the spacer. This side was filled with pure electrolyte solution. On the other side of the spacer, the particle suspension was injected and left to deposit on the functionalized glass plate for 2 h. Subsequently, the suspension was exchanged by the same solution without particles, such that only those particles attached to the substrate remained in the cell. The spacer was then removed and the entire fluid cell was rinsed with the same solution again. One of the colloidal particles was picked up with the functionalized cantilever as described above. The interaction with another similar particle was measured first, and subsequently the force against the silica substrate was recorded.

C. Poisson-Boltzmann (PB) theory

Forces between electric double layers were calculated with PB theory [4,29,30,44]. Provided the particles are sufficiently large, the calculation is substantially simplified with the Derjaguin approximation, carrying out the PB calculations in the plate-plate geometry [4]. We consider two charged plates with an electrolyte solution in between containing different types of ions i of number concentration c_i and charge z_i expressed in units of the elementary charge q. The electric potential $\psi(x)$ depends on the position x, whose origin is taken at the midplane and the two surfaces are located at $x = \pm h/2$. This potential profile can be obtained from the PB equation [30,44],

$$\frac{d^2\psi}{dx^2} = -\frac{q}{\varepsilon_0\varepsilon}\sum_i z_i c_i e^{-z_i\beta q\psi}, \tag{1}$$

where ε_0 is the dielectric permittivity of vacuum, ε the dielectric constant, and $\beta = 1/(kT)$ the inverse thermal energy. The latter relation introduces T as the absolute temperature and k as the Boltzmann constant. We use $\varepsilon = 80$ as appropriate for water at room temperature. The PB equation is solved numerically subject to the constant regulation (CR) boundary conditions

$$\pm\varepsilon_0\varepsilon\frac{d\psi}{dx}\bigg|_{x=\pm h/2} = \sigma^{(\pm)} - C_{\mathrm{I}}^{(\pm)}[\psi(\pm h/2) - \psi_{\mathrm{D}}^{(\pm)}], \tag{2}$$

where the superscript ± refers to the right (+) or left (–) surface, $\psi_{\mathrm{D}}^{(\pm)}$ and $\sigma^{(\pm)}$ denote the diffuse-layer potentials and surface charge densities of the isolated surfaces, and $C_{\mathrm{I}}^{(\pm)}$ their inner layer capacitances. The diffuse-layer potential of an isolated surface is related to the surface charge density by

$$\sigma^{(\pm)} = \pm\left[2k_{\mathrm{B}}T\varepsilon_0\varepsilon\sum_i c_i\left(e^{-z_i\beta q\psi_{\mathrm{D}}^{(\pm)}} - 1\right)\right]^{1/2}, \tag{3}$$

where the ± signs on the right-hand side of the equality sign refer to positive and negative potentials. Instead of the inner layer capacitance, we report the regulation parameter defined as [29,44]

$$p^{(\pm)} = \frac{C_{\mathrm{D}}^{(\pm)}}{C_{\mathrm{D}}^{(\pm)} + C_{\mathrm{I}}^{(\pm)}}, \tag{4}$$

where for either surface the diffuse-layer capacitance is given by

$$C_{\rm D}^{(\pm)} = \frac{\partial \sigma^{(\pm)}}{\partial \psi_{\rm D}^{(\pm)}} = \pm\left(\frac{q^2\varepsilon_0\varepsilon}{2kT}\right)^{1/2} \frac{\sum_i z_i c_i (e^{-z_i\beta q\psi_{\rm D}^{(\pm)}} - 1)}{\left[\sum_i c_i (e^{-z_i\beta q\psi_{\rm D}^{(\pm)}} - 1)\right]^{1/2}}. \tag{5}$$

The regulation parameter provides a more intuitive interpretation of the boundary conditions, since $p^{(\pm)} = 1$ refers to CC conditions, and $p^{(\pm)} = 0$ to CP conditions. In general, the regulation parameter can assume any value $p^{(\pm)} \leqslant 1$, and can in principle become negative [32]. However, the latter situations seem rare. We assume that dissolved ions originate from the dissociation of different electrolytes $A_{\nu_+}B_{\nu_-} \rightarrow \nu_+ A^{z_+} + \nu_- B^{z_-}$ where z_+ and z_- are their charges and ν_+ and ν_- the stoichiometric coefficients. Consideration of mixed electrolytes can be necessary. One should recall that the parameters $\psi_{\rm D}^{(\pm)}$, $\sigma^{(\pm)}$, $C^{(\pm)}$, and $p^{(\pm)}$ refer to the surfaces at infinite separation, and are thus properties of the single, isolated surface. When two surfaces approach, the actual diffuse-layer potentials and the surface charge densities will vary with the separation distance [29,30,44]. For symmetric systems, PB theory predicts that upon approach the magnitude of the diffuse-layer potential increases, while the magnitude of the charge density will decrease. In asymmetric systems, this dependence can be nonmonotonic.

Forces between particles are calculated from the disjoining pressure given by [4,44]

$$\Pi = kT\sum_i c_i (e^{-z_i\beta q\psi} - 1) - \frac{\varepsilon_0\varepsilon}{2}\left(\frac{d\psi}{dx}\right)^2. \tag{6}$$

Once this pressure is known as a function of the separation distance, free energy per unit area W can be calculated by its integration, namely,

$$W(h) = \int_h^\infty \Pi(h')\,dh'. \tag{7}$$

Once this quantity is obtained, the forces between two particles can be found by invoking the Derjaguin approximation [4],

$$F = 2\pi R_{\rm eff} W, \tag{8}$$

where the effective radius is given by

$$R_{\rm eff} = \frac{R_1 R_2}{R_1 + R_2}, \tag{9}$$

where R_1 and R_2 are the radii of the two particles involved (sphere-sphere geometry). When one deals with a planar substrate, one has $R_{\rm eff} = R_1$, where R_1 is the radius of the probe particle attached to the cantilever (sphere-plane geometry).

This PB calculation of the forces is implemented in a least-squares fitting procedure, and the respective parameters can be extracted from the force curves. In the symmetric situation, the diffuse-layer force depends on three parameters, namely, the salt concentration c, the diffuse-layer potential $\psi_{\rm D}$, and the regulation parameter p. In the asymmetric situation, the force depends on five parameters, namely the salt concentration c, the diffuse-layer potentials $\psi_{\rm D}^{(+)}$ and $\psi_{\rm D}^{(-)}$ for the right and left surfaces, and the corresponding regulation parameters $p^{(+)}$ and $p^{(-)}$. In the following, we shall omit the superscripts ±, since it will be clear from the context to which surface one refers. For electrolyte mixtures involving ions of different valences, all respective concentrations of the various electrolytes enter the calculation.

III. RESULTS AND DISCUSSION

Here we present a strategy on how to measure the charging properties of a water-solid interface reliably with the colloidal-probe technique. These charging properties include the diffuse-layer potential $\psi_{\rm D}$ and the regulation parameter p, which depend on the nature of the surface, but also on the solution composition. The present approach relies on a highly charged probe particle. The charging properties of this particle are calibrated by means of force measurements (symmetric sphere-sphere geometry). This particle should typically have a diffuse-layer potential of 30 mV or more. The calibrated probe particle is then used to measure the forces against another colloidal particle (asymmetric sphere-sphere geometry) or a planar surface (sphere-plane geometry). The approach can also be used for weakly charged or uncharged substrates, for which a precise determination of these quantities is normally difficult. The sign of the surface charge can equally be inferred. Moreover, the technique also works in salt solutions containing multivalent ions. The presented methods also permit us to verify the correctness of the determined quantities independently. However, the verification strategy for colloidal particles and for planar substrates differs. Therefore, we will first discuss the measurement of the charging parameters for colloidal particles, and subsequently we address planar substrates.

A. Colloidal particles and monovalent ions

Let us introduce the technique through the example shown in Fig. 1 (left). We investigate the AL particles of 1.0 μm in diameter suspended in 3.0 mM KCl electrolyte solution adjusted to pH 4.0. These particles are immobilized in the respective solution on a functionalized substrate in an AFM-fluid cell. To obtain the surface properties of these particles, we first carry out force measurements with a SL particle 3.0 μm in diameter. A suspension of these particles is injected to a second compartment of the same fluid cell, and they are also immobilized to the substrate. One of these particles is attached to a functionalized tipless cantilever. We first determine the charging properties of the probe particles, by carrying force measurement between two SL particles in the symmetric geometry [Fig. 1(a), left]. Since the system is symmetric, the double-layer force is repulsive, and the profile can be well fitted with PB theory with CR boundary conditions at distances larger than about 5 nm. At shorter distances, effects of van der Waals and hydrophobic forces become important. One extracts the diffuse-layer potential $\psi_{\rm D} = -71$ mV and the regulation parameter of $p = 0.40$. Both parameters refer to surfaces at larger separation (i.e., isolated surface), and they are summarized in Table II. The sign of the potential for one probe particle must be determined independently, for example, by noting that negatively charged sulfate groups are present on the surface.

We now measure the forces in the asymmetric geometry between the SL probe particle and an AL particle to be investigated [Fig. 1(b), left]. The measured force profile is fitted

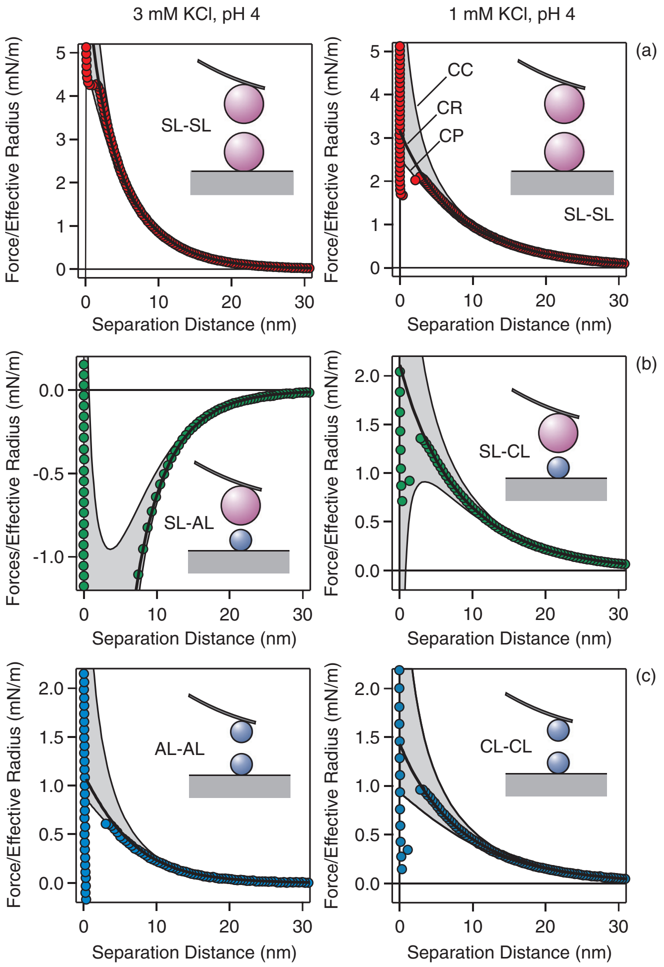

FIG. 1. (Color online) Determination of charging properties by direct force measurements between colloidal particles at pH 4.0 with PB theory invoking constant regulation (CR) conditions. SL is used as the probe particle. The colloidal particles to be investigated are (left column) AL in 3.0 mM KCl solution and (right column) CL in 1.0 mM KCl. The results for constant charge (CC) and constant potential (CP) conditions are indicated as well, and the region in between is shaded. (a) Calibration of the SL probe particle in the symmetric geometry, (b) measurement of the particle to be investigated in the asymmetric geometry, and (c) verification of the results in the symmetric geometry. The parameters are summarized in Tables II and III.

with the PB theory, whereby the charging parameters of the SL particle are fixed to the values determined in the symmetric experiment. We now obtain the charging parameters for the AL particle surface, namely a diffuse-layer potential $\psi_{\mathrm{D}} = +33$ mV and a regulation parameter of $p = 0.22$. Since the forces are attractive, the surface of the AL particle must be positively charged. With the probe particle, the sign of the surface charge can be determined unambiguously. The determination of this sign is impossible in the symmetric experiment.

By measuring forces in the symmetric and asymmetric geometries with the same probe particle, we can determine the charging parameters of an unknown particle to good confidence. The accuracy of the present approach can be verified independently by extracting the charging parameters from the forces between two AL particles in the symmetric geometry. The respective force profile is shown in Fig. 1(c) (left) and the resulting fitted parameters include the diffuse-layer potential $\psi_{\mathrm{D}} = +32$ mV and a regulation parameter of $p = 0.2$ (Table III). One observes very good agreement with the values determined by means of the probe particle. This agreement provides a strong confirmation of the correctness of the technique proposed. The agreement between the surface properties of the AL particle further demonstrates that these properties remain unchanged in the course of the experiment and are independent of the nature of particles in their neighborhood. By reversing the role of the probe and unknown particle, one can also demonstrate that the same applies to the SL particle.

Consideration of charge regulation is essential, however. The effects of the boundary conditions are indicated in Fig. 1 by the gray region, which is limited by the profiles calculated for CC and CP conditions. One observes that such charge regulation effects can be substantial, especially in the asymmetric systems.

Table II summarizes the fitted charging parameters and the errors for the probe particles, while Table III compiles the analogous information for the unknown particles and substrates studied. The errors for the symmetric systems represent estimates of the standard deviations of the mean for three independent repetitions of the same experiment with three different particles attached to the substrate. Thereby, the probe particle was kept the same. The error bars for asymmetric systems were determined in the same way, but they also include the contribution from the error propagation resulting from the errors in the charging parameters of the probe particle. When the present technique is used, the error bars of the potentials are determined by a relative error of about 10% or an absolute error of 2 mV, whichever value leads to a larger absolute error. The error bars of the regulation parameters are about 0.03. The deviations between the fitted and nominal salt concentrations are always small, typically $<10\%$, and we always use the fitted concentrations in the calculations. When the nominal concentrations are used in the fit, the resulting surface potentials and regulations fall within the error bars of the values obtained when the fitted concentrations are used.

Let us now use the same technique for the determination of charging properties of CL particles. Such particles are highly charged in basic solution, and they become almost neutral in acidic conditions [36]. This system will illustrate the main advantage of the present technique, namely, that one can reliably measure the charging parameters for surfaces that are close to electrically neutral.

Let us focus on the situation when the CL particles are highly charged first. The conditions chosen are 1.0 mM KCl solution and pH 4.0. Figure 1(a) (right) shows the force profile for the symmetric system that is used for the calibration of the SL probe particle. Least-squares fit yields a diffuse-layer potential $\psi_{\mathrm{D}} = -66$ mV and the regulation parameter of $p = 0.25$ (Table II). The forces in the asymmetric system involving the SL and CL particles shown in Fig. 1(b) (right) are also repulsive, which indicates that the charge of the carboxyl particle is negative. By fixing the charging parameters of SL particles, the least-squares fit of the force profile yields for the CL particle $\psi_{\mathrm{D}} = -42$ mV and the regulation parameter

TABLE II. Calibration of probe particles in different salt solutions in the symmetric sphere-sphere geometry.

Probe particle	Added salt	Concentration (mM)	*p*H	Diffuse-layer potential[a] ψ_D (mV)	Regulation parameter[a] p
SL	KCl	3.0	4.0	-71 ± 3	0.40 ± 0.03
SL	KCl	1.0	4.0	-66 ± 3	0.25 ± 0.02
SL	KCl	0.1	3.0	-58 ± 3	0.31 ± 0.06
SL	KCl	1.0	3.0	-53 ± 2	0.32 ± 0.05
SL	K_2SO_4	1.5	4.0	-46 ± 3	0.27 ± 0.07
AL	$LaCl_3$	0.80	4.0	$+40 \pm 3$	0.31 ± 0.03
SL	KCl	2.0	3.0	-60 ± 2	0.31 ± 0.05
AL	KCl	2.0	3.0	$+59 \pm 3$	0.37 ± 0.05

[a] These parameters refer to the isolated surface. The error refers to the standard deviation, and is based on force measurements between at least three pairs of particles.

of $p = 0.37$. To verify the validity of the approach, we also estimate these parameters from the force profile between two CL particles in the symmetric experiment. Figure 1(c) (right) shows the corresponding force profile, and yields the best fit parameters of $\psi_D = -42$ mV and $p = 0.38$. The parameters are also compared in Table III. Their values are the same within experimental error, which provides further confidence in the present approach.

The examples considered so far focused on situations where both particles were highly charged. In this situation, it was equally possible to directly extract the charging characteristics from the force measurements on the symmetric systems. When the particles are close to neutral, however, the electrostatic force becomes weak, and this approach is no longer feasible. With a highly charged probe particle, however, one can still reliably estimate the charging properties of weakly charged particles accurately. Let us illustrate such cases in the following.

Such situations occur for CL particles at *p*H 3.0 and they are shown in Fig. 2. Let us first discuss the case when only 0.1 mM KCl electrolyte is added. Figure 2(a) (left) shows the calibration force profiles of the SL probe particle that is used to obtain its charging properties. This particle is highly charged, and the charging parameters can be determined reliably (Table II). Least-squares fit in the asymmetric system yield diffuse-layer potentials of $\psi_D = -13$ mV and $p = 0.46$. To test the reliability of these results, we fit force curves between two CL particles in the symmetric situation. This force is now very weak, but the resulting parameters $\psi_D = -13$ mV and $p = 0.4$ are still in good agreement with the probe particle approach. Table III compares these values. Nevertheless, the errors bars in the symmetric system are larger, and the values

TABLE III. Charging properties of surfaces of isolated particles and planar substrates in different salt solutions.

Surface investigated	Added salt	Concentration (mM)	*p*H	Probe particle	Diffuse-layer potential ψ_D (mV)	Regulation parameter p
AL	KCl	3.0	4.0	SL[a]	$+33 \pm 3$	0.22 ± 0.08
				AL[b]	$+32 \pm 3$	0.2 ± 0.1
CL	KCl	1.0	4.0	SL[a]	-42 ± 3	0.37 ± 0.03
				CL[b]	-42 ± 3	0.38 ± 0.03
CL	KCl	0.10	3.0	SL[a]	-13 ± 2	0.46 ± 0.02
				CL[b]	-13 ± 2	0.4 ± 0.2
CL	KCl	1.0	3.0	SL[a]	-9 ± 1	0.44 ± 0.03
				CL[b]	-7 ± 2	—[c]
AL	K_2SO_4	1.5	4.0	SL[a]	$+22 \pm 3$	0.27 ± 0.03
				AL[b]	$+20 \pm 5$	0.33 ± 0.07
SL	$LaCl_3$	0.80	4.0	AL[a]	-6 ± 1	0.11 ± 0.03
				SL[b]	-3 ± 2	—[c]
Silica[d]	KCl	2.0	3.0	SL	-13 ± 1	0.33 ± 0.02
				AL	-13 ± 2	0.31 ± 0.03

[a] Asymmetric sphere-sphere geometry with the probe particle indicated. The errors refer to the standard deviation. They are based on force measurements between at least three pairs of particles and include error propagation due to the uncertainties of the charging properties of the probe particle.

[b] Symmetric sphere-sphere geometry measured with the same type of particle as the one investigated. The errors refer to the standard deviation. They are based on force measurements between at least three pairs of particles.

[c] The regulation parameter could not be determined from the fit.

[d] Planar silica substrate measured in the asymmetric sphere-plane geometry with two different probe particles.

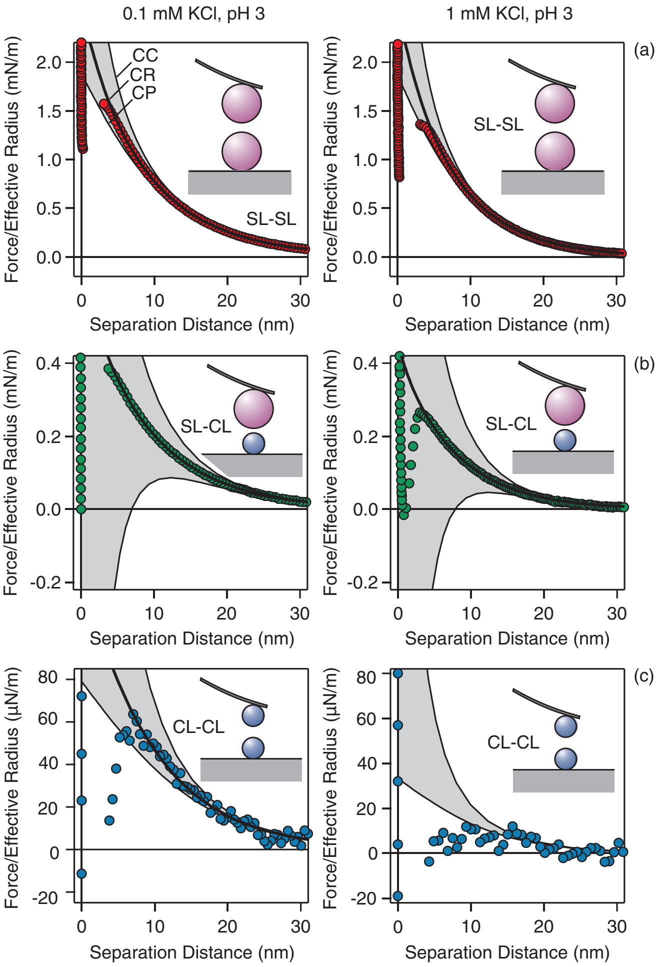

FIG. 2. (Color online) Determination of charging properties by direct force measurements of CL particles at pH 3.0 with PB theory invoking constant regulation (CR) conditions. SL probe particle is used in (left column) 0.1 mM KCl solution and (right column) 1.0 mM KCl solution. The results for constant charge (CC) and constant potential (CP) conditions are indicated as well, and the region in between is shaded. (a) Calibration of the SL probe particle in the symmetric geometry, (b) measurement of the CL particle to be investigated in the asymmetric geometry, and (c) verification of the results in the symmetric geometry. In the latter symmetric case, the forces are so weak that the complete determination of the charging properties becomes impossible. For this reason, only the CC and CP conditions are used. The parameters are summarized in Table II and III.

obtained by means of the probe particle are definitely more accurate.

The real advantage of the present probe particle technique becomes obvious when one investigates the CL particles at pH 3.0 when 1.0 mM KCl electrolyte has been added. This approach yields for the CL particle the charging parameters of $\psi_D = -9$ mV and $p = 0.44$ [Figs. 2(a) and 2(b), right]. To extract both parameters from the forces between the CL particles is now impossible [Fig. 2(c), right]. Since the forces are very weak, the noise is substantial. The regulation parameter cannot be determined, but the diffuse-layer potential can be estimated to be roughly $\psi_D = -7$ mV (Table III). In this case, the present technique is clearly superior to force measurements in the symmetric situation.

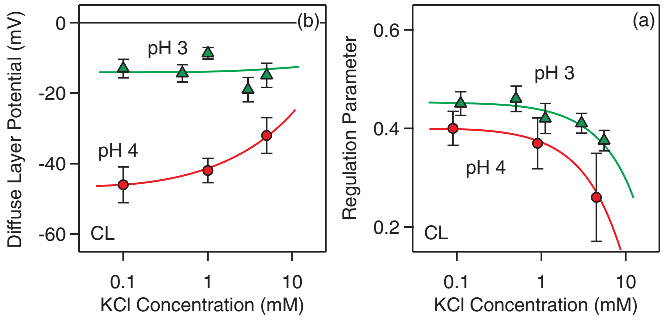

FIG. 3. (Color online) Measured charging parameters of CL particles versus the added salt KCl concentration at pH 3.0 and 4.0. These values are partially reported in Table III. Solid lines are only shown to guide the eye. (a) Diffuse-layer potentials and (b) regulation parameters.

The necessity to consider the regulation properties of the interfaces involved should be fully obvious at this point. Inspection of Fig. 2 reveals that the gray areas, which indicate the influence of different charge regulation conditions, extend over wide regions. This influence is particularly pronounced in the asymmetric case, and for this reason these force profiles are much more sensitive to the charge regulation parameter than the symmetric ones. The constant regulation (CR) approximation provides a simple way to quantify these regulation properties consistently.

Figure 3 summarizes the diffuse-layer potentials and the regulation parameters of the CL particle surfaces, which were measured at additional solution compositions. In spite of the low potentials of the CL particles, this technique provides accurate values of the diffuse-layer potentials and the regulation parameters. One observes that the magnitude of the potential decreases with increasing salt concentration. This behavior is in agreement with classical PB theory. Its magnitude also increases with increasing pH, which is caused by the larger fraction of dissociated carboxylic surface groups. The regulation parameter also shows a weak dependence on the salt concentration, but the present technique suggests that its value also decreases with increasing pH and salt concentration. While this pH dependence is in qualitative agreement with predictions of the simple diffuse-layer model, the same model predicts the reverse trends for the salt dependence of this parameter [45]. The latter disagreement probably originates from the specific adsorption of simple electrolyte ions to the particle surface.

The present technique works best at low salt concentrations, and its reliability decreases with increasing salt level. The current limit of applicability is roughly around 10 mM. At higher salt levels, the forces become short ranged and other forces besides double-layer forces become important. By including van der Waals forces in the analysis, one should be able to extent its applicability to higher salt concentrations. This approach might be feasible by exploring forces at larger distances, but in this case the regulation properties cannot be determined [34]. At the same time, however, the force and distance resolution may become critical, since under these conditions the forces become weak.

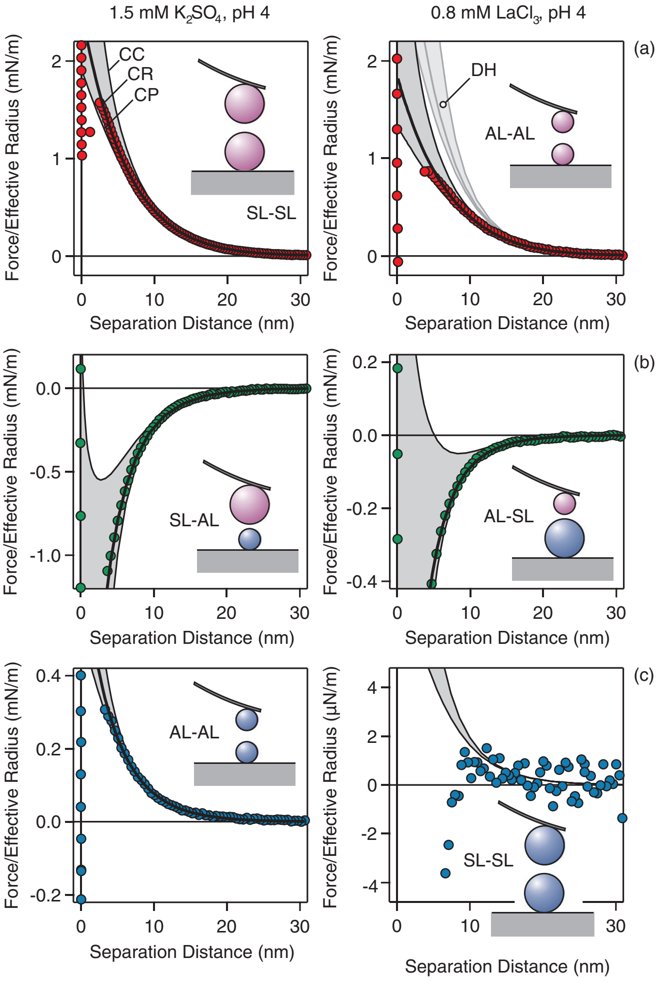

FIG. 4. (Color online) Determination of charging properties by direct force measurements in electrolyte solutions containing multivalent ions at pH 4.0 with PB theory invoking constant regulation (CR) conditions. AL particles measured with a SL probe particle in 1.5 mM K_2SO_4 solution (left column). SL particles measured with an AL probe particle in 0.8 mM $LaCl_3$ solution (right column). The results for constant charge (CC) and constant potential (CP) conditions are indicated as well, and the region in between is shaded. (a) Calibration of the probe particle in the symmetric geometry, (b) measurement of the particle to be investigated in the asymmetric geometry, and (c) verification of the results in the symmetric geometry. In the latter symmetric case in $LaCl_3$ solution, the weak forces make a complete determination of the charging properties possible. The parameters are summarized in Tables II and III. The left (a) panel shows for comparison the respective calculation of Debye-Hückel (DH) theory with the same long distance decay as PB theory.

B. Colloidal particles and multivalent ions

The present probe particle technique is equally applicable in salt solutions containing multivalent ions. However, the PB theory must be extended to the appropriate asymmetric electrolytes and, if necessary, to their mixtures. Figure 4 shows two respective examples.

Let us first discuss the situation in 1.5 mM K_2SO_4 electrolyte at pH 4.0 where the charging parameters of the AL particles are determined. We choose a SL particle as the probe, which is highly charged in this medium, since the divalent sulfate ions interact with the negatively charged surface only weakly. From the symmetric force profile, one obtains the charging parameters given in Table II [Fig. 4(a), left]. The PB theory used considers the fact that the electrolyte contains monovalent and divalent anions. In the asymmetric situation, one can now extract the surface properties of the AL particle as $\psi_D = +22$ mV and the regulation parameter of $p = 0.27$ [Fig. 4(b), left]. When one carries out the measurement with AL particles in the symmetric situation, one finds $\psi_D = +20$ mV and $p = 0.33$ [Fig. 4(c), left]. These parameters are also summarized in Table III. This experiment thus confirms that the technique works equally well in the presence of multivalent ions.

Similar experiments are now carried out in 0.8 mM $LaCl_3$ electrolyte at pH 4.0. In this medium, the SL becomes weakly charged, due to strong adsorption of the trivalent lanthanum ions. Now we choose an AL particle as the probe, since these particles remain highly charged in this medium, as the multivalent lanthanum ions hardly interact with the positively charged surface. They can thus be calibrated easily, and we obtain the charging parameters shown in Table II [Fig. 4(a), right]. The PB theory now includes the presence of monovalent and trivalent cations. The charging properties of the SL particle can be again accurately determined in the asymmetric situation and one finds $\psi_D = -6$ mV and $p = 0.11$ [Fig. 4(b), right]. When one attempts to interpret the force profile between the SL particles, the noise is substantial, and it is not possible to determine the regulation parameter [Fig. 4(c), right]. Nevertheless, one may still obtain a rough estimate of the diffuse-layer potential $\psi_D = -3$ mV. This value agrees reasonably well with the value determined in the asymmetric system (Table III).

When the surface to be investigated is weakly charged, it is no longer possible to extract the regulation parameter from the symmetric experiment, while the probe particle approach reveals the precise value of this parameter easily. The effect of charge regulation is again very important in the asymmetric system. A similar situation was encountered with the CL particle at pH 3.0 in 1.0 mM KCl solution [Fig. 2(c), right]. One should note that the fitted concentration of the $LaCl_3$ solution is about 15% lower than the nominal value. We suspect that this deviation is due to formation of $LaCl^{2+}$ complexes [9,46].

While the present technique also works reliably in the presence of multivalent ions, it is essential that the data analysis is carried out with the nonlinear PB equation for the appropriate electrolyte composition. The use of the Debye-Hückel (DH) approximation or simplifications to symmetric electrolytes may be grossly inaccurate. This point is illustrated in Fig. 4(a) (right) where we show the corresponding force curve from the DH approximation, which is obtained by linearizing the PB equation. While DH theory is correct at larger distances, it performs poorly at shorter distances, especially in the presence of multivalent coions, where the full PB description becomes essential. The reasons for these deviations discussed in more detail elsewhere [44].

C. Planar substrate

The same technique can also be used to determine charging parameters of planar substrates. In this situation, it is

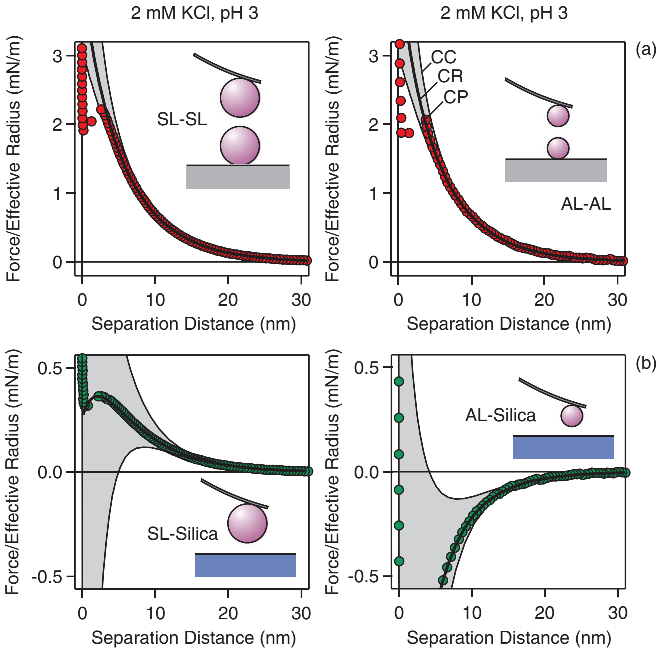

FIG. 5. (Color online) Determination of charging properties by direct force measurements of a planar silica substrate with PB theory invoking constant regulation (CR) conditions at pH 3.0 in 2.0 mM KCl electrolyte solution. Probe particles used are (left column) SL and (right column) AL. The results for constant charge (CC) and constant potential (CP) conditions are indicated as well, and the region in between is shaded. (a) Calibration of the probe particles in the symmetric geometry, (b) measurement of the forces between probe particle and the planar silica substrate. The parameters are summarized in Tables II and III.

impossible to carry out the respective measurement in the symmetric system. There were several attempts to mimic a symmetric system in the sphere-plane geometry, for example, by choosing a colloidal probe with a similar composition as the planar substrate or by appropriate surface coatings [47–49]. However, the realization of such a system can be challenging, and the symmetry of such a setting can never be proven. This difficulty can be easily circumvented with the probe particle technique, and the correctness of the measured values can be further verified by repeating the measurements with different probe particles.

Figure 5 shows the corresponding experiment, where the charging properties of a planar silica substrate were determined. The substrate is a silicon wafer, which is coated by a silica layer by spontaneous oxidation in air. This experiment was carried out in a 2.0 mM KCl solution adjusted to pH 3.0. We first choose a SL particle as the probe. The force profile was fitted to the PB model and the resulting charging parameters are summarized in Table II [Fig. 5(a), left]. The force between the SL particle and the planar silica substrate was then measured, and the least-squares fit yields a diffuse-layer potential of $\psi_D = -13$ mV and a regulation parameter of $p = 0.33$ [Fig. 5(b), left]. The reliability of these numbers can be verified with another type of probe particle, and for this purpose an AL particle is chosen as the probe. After calibrating the charging characteristics of this particle given in Table II [Fig. 5(a), right], the measurement involving the silica substrate yields $\psi_D = -13$ mV and the regulation parameter of $p = 0.31$ [Fig. 5(b), right]. These numbers determined with the different probe particles are also compared in Table III, and one finds that they are in excellent agreement. The probe particle technique thus also yields reliable values for the charging properties of planar substrates.

IV. CONCLUSION

The present article shows how the combination of the colloidal-probe technique with PB theory provides a powerful framework to reliably determine the charging properties of spherical particles or planar substrates. The principal idea is to perform direct force measurements with the AFM with a previously calibrated, highly charged probe particle and the surface in question. This setting permits to reliably determine diffuse-layer potentials and regulation parameters even in situations where the surface to be investigated is close to neutral. In this fashion, one can determine the diffuse-layer potentials of a few millivolts to good accuracy, including their sign. One can further measure the regulation properties even of neutral substrates. The same approach can also be used in the presence of multivalent ions. This probe particle technique can be used to analyze surface properties of a wide range of substrates and media. In favorable cases, the technique confirms that the determined charging parameters are consistent and independent of the type of the probe used.

In spite of these advantages, the technique also has two important disadvantages. First, it can only be used for moderately large colloidal particles. Here we handle particles of 1 μm in diameter, and the same approach can be probably extended to somewhat smaller particles. Substantially smaller particles, which are no longer visible in the optical microscope, cannot be used, since the entire attachment and centering procedure is no longer feasible. Second, the technique can only be used up to moderately high salt levels, typically 10 mM. At higher levels, the forces become too weak and too short ranged to be reliably interpreted. Under these conditions, additional forces contribute to the force profile, in particular, van der Waals and hydrophobic interactions. These forces complicate the unambiguous data interpretation, which was presented here. Some progress might be possible by including van der Waals forces in the analysis and eventually by focusing on larger distances, but sacrificing the possibility to obtain information on charge regulation. The technique could probably be extended by including additional types of forces in the data analysis to smaller particles and to higher salt levels, especially with modern AFMs offering improved force resolution.

ACKNOWLEDGMENTS

This research was supported by the Swiss National Science Foundation, University of Geneva, COST Action No. CM1101, and the Swiss Secretariat of Education and Research.

[1] A. P. Hynninen, J. H. J. Thijssen, E. C. M. Vermolen, M. Dijkstra, and A. van Blaaderen, Nat. Mater. **6**, 202 (2007).

[2] B. Balzer, M. K. M. Hruschka, and L. J. Gauckler, J. Colloid Interface Sci. **216**, 379 (1999).

[3] A. Wolthoorn, E. J. M. Temminghoff, and W. H. van Riemsdijk, Appl. Geochem. **19**, 1391 (2004).

[4] W. B. Russel, D. A. Saville, and W. R. Schowalter, *Colloidal Dispersions* (Cambridge University Press, Cambridge, 1989).

[5] E. E. Meyer, K. J. Rosenberg, and J. Israelachvili, Proc. Natl. Acad. Sci. USA **103**, 15739 (2006).

[6] I. Szilagyi, G. Trefalt, A. Tiraferri, and M. Borkovec, Soft Matter **10**, 2479 (2014).

[7] P. Sinha, I. Szilagyi, F. J. Montes Ruiz-Cabello, P. Maroni, and M. Borkovec, J. Phys. Chem. Lett. **4**, 648 (2013).

[8] J. Forsman, J. Phys. Chem. B **108**, 9236 (2004).

[9] C. F. Baes and R. E. Mesmer, *The Hydrolysis of Cations* (Krieger Publishing, Malabar, FL, 1976).

[10] W. D. Schecher and D. C. McAvoy, Comput. Environ. Urban Syst. **16**, 65 (1992).

[11] M. Delhorme, C. Labbez, C. Caillet, and F. Thomas, Langmuir **26**, 9240 (2010).

[12] C. Labbez, B. Jonsson, I. Pochard, A. Nonat, and B. Cabane, J. Phys. Chem. B **110**, 9219 (2006).

[13] T. Hiemstra, Langmuir **28**, 15614 (2012).

[14] E. Trizac, L. Bocquet, and M. Aubouy, Phys. Rev. Lett. **89**, 248301 (2002).

[15] J. Israelachvili, Y. Min, M. Akbulut, A. Alig, G. Carver, W. Greene, K. Kristiansen, E. Meyer, N. Pesika, K. Rosenberg, and H. Zeng, Rep. Prog. Phys. **73**, 036601 (2010).

[16] R. M. Espinosa-Marzal, T. Drobek, T. Balmer, and M. P. Heuberger, Phys. Chem. Chem. Phys. **14**, 6085 (2012).

[17] G. Binnig, C. F. Quate, and C. Gerber, Phys. Rev. Lett. **56**, 930 (1986).

[18] W. A. Ducker, T. J. Senden, and R. M. Pashley, Nature **353**, 239 (1991).

[19] H. J. Butt, Biophys. J. **60**, 1438 (1991).

[20] H. J. Butt, B. Cappella, and M. Kappl, Surf. Sci. Rep. **59**, 1 (2005).

[21] H. H. von Grunberg, L. Helden, P. Leiderer, and C. Bechinger, J. Chem. Phys. **114**, 10094 (2001).

[22] G. Toikka, R. A. Hayes, and J. Ralston, Langmuir **12**, 3783 (1996).

[23] S. Rentsch, R. Pericet-Camara, G. Papastavrou, and M. Borkovec, Phys. Chem. Chem. Phys. **8**, 2531 (2006).

[24] I. Popa, P. Sinha, M. Finessi, P. Maroni, G. Papastavrou, and M. Borkovec, Phys. Rev. Lett. **104**, 228301 (2010).

[25] J. C. Crocker and D. G. Grier, Phys. Rev. Lett. **73**, 352 (1994).

[26] C. Gutsche, U. F. Keyser, K. Kegler, F. Kremer, and P. Linse, Phys. Rev. E **76**, 031403 (2007).

[27] J. Baumgartl, J. L. Arauz-Lara, and C. Bechinger, Soft Matter **2**, 631 (2006).

[28] S. L. Carnie and D. Y. C. Chan, J. Colloid Interface Sci. **161**, 260 (1993).

[29] S. H. Behrens and M. Borkovec, Phys. Rev. E **60**, 7040 (1999).

[30] R. Pericet-Camara, G. Papastavrou, S. H. Behrens, and M. Borkovec, J. Phys. Chem. B **108**, 19467 (2004).

[31] M. Lund and B. Jonsson, Biochemistry **44**, 5722 (2005).

[32] M. Borkovec and S. H. Behrens, J. Phys. Chem. B **112**, 10795 (2008).

[33] O. Zohar, I. Leizerson, and U. Sivan, Phys. Rev. Lett. **96**, 177802 (2006).

[34] M. Elzbieciak-Wodka, M. Popescu, F. J. Montes Ruiz-Cabello, G. Trefalt, P. Maroni, and M. Borkovec, J. Chem. Phys. **140**, 104906 (2014).

[35] M. Borkovec, S. H. Behrens, and M. Semmler, Langmuir **16**, 5209 (2000).

[36] S. H. Behrens, D. I. Christl, R. Emmerzael, P. Schurtenberger, and M. Borkovec, Langmuir **16**, 2566 (2000).

[37] R. W. O'Brien and L. R. White, J. Chem. Soc., Faraday Trans. 2 **74**, 1607 (1978).

[38] A. V. Delgado, F. Gonzalez-Caballero, R. J. Hunter, L. K. Koopal, and J. Lyklema, J. Colloid Interface Sci. **309**, 194 (2007).

[39] R. J. Hill, D. A. Saville, and W. B. Russel, J. Colloid Interface Sci. **268**, 230 (2003).

[40] V. Lobaskin, B. Dunweg, M. Medebach, T. Palberg, and C. Holm, Phys. Rev. Lett. **98**, 176105 (2007).

[41] J. L. Anderson, J. Colloid Interface Sci. **105**, 45 (1985).

[42] M. Finessi, P. Sinha, I. Szilagyi, I. Popa, P. Maroni, and M. Borkovec, J. Phys. Chem. B **115**, 9098 (2011).

[43] I. Popa, G. Gillies, G. Papastavrou, and M. Borkovec, J. Phys. Chem. B **113**, 8458 (2009).

[44] G. Trefalt, I. Szilagyi, and M. Borkovec, J. Colloid Interface Sci. **406**, 111 (2013).

[45] S. H. Behrens and M. Borkovec, J. Phys. Chem. B **103**, 2918 (1999).

[46] A. E. Martell, R. M. Smith, and R. J. Motekaitis, *Critically Selected Stability Constants of Metal Complexes: Version 8.0* (National Institute of Standards and Technology, Gaithersburg, MD, 2004).

[47] S. Leporatti, R. Sczech, H. Riegler, S. Bruzzano, J. Storsberg, F. Loth, W. Jaeger, A. Laschewsky, S. Eichhorn, and E. Donath, J. Colloid Interface Sci. **281**, 101 (2005).

[48] P. G. Hartley, I. Larson, and P. J. Scales, Langmuir **13**, 2207 (1997).

[49] S. Biggs, P. Mulvaney, C. F. Zukoski, and F. Grieser, J. Am. Chem. Soc. **116**, 9150 (1994).